Available online at www.sciencedirect.com
SCIENCE DIRECT
Talanta 67 (2005) 472–478
Talanta
www.elsevier.com/locate/talanta

Quantum dots-based reverse phase protein microarray

Masato Shingyoji [a], Daniele Gerion [b], Dan Pinkel [c], Joe W. Gray [a,c], Fanqing Chen [a,*]

[a] *Life Sciences Division, Lawrence Berkley National Laboratory, University of California at Berkeley, MS 977R0225A, 1 Cyclotron Road, Berkeley, CA 94720, USA*
[b] *Physics and Advanced Technology, Lawrence Livermore National Laboratory, Livermore, CA 94551, USA*
[c] *Department of Laboratory Medicine and the Comprehensive Cancer Center, University of California, San Francisco, CA 94143, USA*

Abstract

CdSe nanocrystals, also called quantum dots (Qdots) are a novel class of fluorophores, which have a diameter of a few nanometers and possess high quantum yield, tunable emission wavelength and photostability. They are an attractive alternative to conventional fluorescent dyes. Quantum dots can be silanized to be soluble in aqueous solution under biological conditions, and thus be used in bio-detection. In this study, we established a novel Qdot-based technology platform that can perform accurate and reproducible quantification of protein concentration in a crude cell lysate background. Protein lysates have been spiked with a target protein, and a dilution series of the cell lysate with a dynamic range of three orders of magnitude has been used for this proof-of-concept study. The dilution series has been spotted in microarray format, and protein detection has been achieved with a sensitivity that is at least comparable to standard commercial assays, which are based on horseradish peroxidase (HRP)-catalyzed diaminobenzidine (DAB) chromogenesis. The data obtained through the Qdot method has shown a close linear correlation between relative fluorescence unit and relative protein concentration. The Qdot results are in almost complete agreement with data we obtained with the well-established HRP–DAB colorimetric array ($R^2 = 0.986$). This suggests that Qdots can be used for protein quantification in microarray format, using the platform presented here.
Published by Elsevier B.V.

Keywords: Quantum dots; Protein microarray; Bioconjugation; Tyramide signal amplification; Reverse phase protein lysate microarray; DNA-PK

1. Introduction

The in vitro analysis of extracted cellular proteins may give a wealth of information on their expression level, modification, degradation, complex formation, activity, and localization. One of such analyses is the high-throughput measurement allowed by patterning the protein in a microarray format [1–5]. The proteins can be covalently linked to or immobilized by high-capacity absorption on a substrate surface, then detected with immunochemistry. In fact, microarrays were developed in the 1990s for genomic studies, where the massive parallel output afforded by the microarray has greatly improved the speed and scope of gene expression analysis and genotyping [6–11], to the point where DNA microarrays are now a routine analytical tool in genomics studies. By contrast, protein microarrays have not witnessed the same impressive popularity, mainly because the adsorption chemistry of the proteins onto the surface poses many challenges, and no convenient detection mechanism has yet become firmly established [5]. Detection of proteins depends mainly on the specificity and affinity of the antibodies. In general, antibodies are expensive to generate, they lack consistency in affinity and specificity, correspond only to individual proteins, and they are available only for a fraction of the proteins in the proteome [5]. Moreover, the protein has to expose its epitopes so as to be accessible by the targeting probes, such as antibodies and aptamers. These problems have retarded the widespread use of protein microarrays.

Yet, in the past few years, protein microarrays have made steady progress and have come of age. However, one challenge remains. The most popular detection method uses fluorescence detection by specifically labeling the adsorbed proteins [4]. Conventional dyes currently present several shortcomings. First, their level of detection permits a lower detection threshold in the picomolar range in regular biolog-

* Corresponding author. Tel.: +1 510 495 2444; fax: +1 510 486 5586.
E-mail address: f_chen@lbl.gov (F. Chen).

0039-9140/$ – see front matter. Published by Elsevier B.V.
doi:10.1016/j.talanta.2005.06.064

ical assay conditions. Second, their relatively large emission pattern (>50 nm) poses certain problems for multiplex detections when the signals are low, because filtering out the cross-talks between channels comes at the expense of the signal intensity. Therefore, there is an urgent need to develop detection techniques that do not rely on organic dyes.

Recently, reverse phase protein lysate microarrays have been reported, in which cell lysate proteins are immobilized on nitrocellulose-coated substrate, while a dilution series of the lysates with a dynamic range of at least 1000-fold is used for quantification of protein [12]. This method assesses only one protein per microarray, but it nonetheless has a great advantage because multiple samples can be analyzed and compared side by side in a single array [13,14]. Proteins on a microarray are detected with a highly effective signal amplification procedure, involving horseradish peroxidase (HRP)-catalyzed diaminobenzidine (DAB) chromogenesis. DAB is a commonly used chromogen with HRP. This amplification system is based on catalyzed reporter deposition of biotinylated tyramide [15–18]. The combination of DAB and tyramide signal amplification (TSA) results in a brown precipitate with excellent signal-to-noise ratio [12]. Using the HRP–DAB platform, detection of proteins in single cell can be accomplished routinely [13]. However, the HRP–DAB system is sensitive to various factors, such as temperature, reagent quality, and specific activity of the HRP enzyme.

We investigate here the use of fluorescent semiconductor quantum dots (Qdots) as an alternative visualization label for protein microarray studies [19]. Qdots are crystalline materials made of a CdSe core of a few nanometers, and surrounded by a thin shell of ZnS [20]. This CdSe/ZnS core/shell nanostructure has the ability to emit light upon UV excitation. The emission is narrow (∼20–25 nm fwhm) and can be tuned by adjusting the size of the CdSe core, due to the quantum confinement effect. The colloidal chemistry is so well developed that it allows the synthesis of five to six spectrally distinct colors of emission across the visible spectrum [10]. Recent progress in synthesis has allowed the highly efficient conjugation of the CdSe/ZnS nanocrystals to a wide variety of biomolecules such as DNA [21,22], proteins [23], antibodies [24,25], or short peptides [26]. Several years ago, we successfully adapted the Qdot technology for the study of cDNA microarrays [8]. By devising a highly efficient means to achieve Qdot–DNA linkage, we showed that single nucleotide polymorphism detection of genomic DNA could be reached within minutes, at room temperature, with true-to-false signal ratios above 10 [8]. This was due to the fact that non-specific binding was totally suppressed by working in hostile conditions for the DNA–DNA binding, where only the perfect complements have a stable interaction. We have been intrigued by the possibility of finding out if a similar use of Qdots can be found in protein arrays.

We present here a study of protein microarray using TSA and fluorescent Qdots coupled with streptavidin. We used a protein called DNA-dependent protein kinase catalytic subunit (DNA-PKcs) as our target. DNA-PKcs is a large protein of 465 kDa, and difficult to detect even by Western blot [27,28]. Cell lysates spiked with DNA-PK proteins were arrayed in high density in serial dilution and detected with a monoclonal antibody derived from a hybridoma cell line. We performed assays on the reversed phase protein lysate arrays using both the conventional HRP–DAB method and our novel streptavidin–Qdot-based method. The Qdot-based method has shown promising results in comparison to the enzymatic colorimetric method. The relative fluorescence unit (RFU) data obtained through the Qdot method has shown a close linear correlation with relative protein concentration on a logarithmic scale. The Qdot result has shown close agreement with the data we obtained with the well-established HRP–DAB colorimetric protein array method ($R^2 = 0.986$). This suggests that Qdots can be used for protein quantification in high-density microarray format, using the platform presented here (Fig. 1).

2. Materials and methods

2.1. Preparation and dilution of protein lysate

The DNA-PKcs-deficient human glioma cell line M059J [29] was cultured in 5% CO_2 in DMEM media supplemented with 10% fetal calf serum and antibiotics [27]. The DNA-PKcs protein was kindly provided by Dr. Scott R. Peterson and prepared as described before [30]. For protein lysate microarrays, the cultured cells were collected by scraping, and protein lysates were prepared from the cells according to the procedure of Nishizuka et al. [31]. Briefly, cells were collected by scraping and washed three times with cold PBS. The resulting pellets were lysed in buffer containing 9 M urea (Sigma, MO, USA), 4% 3-[(3-cholamidopropyl)dimethylammonio]-1-propanesulfonate (CHAPS; Calbiochem, CA, USA), 2% pH 8.0–10.5 Pharmalyte (Amersham Pharmacia Biotech, Piscataway, NJ, USA), and 65 mM DTT (Amersham Pharmacia Biotech, USA). After lysis, the samples were centrifuged briefly, and the supernatants were stored at −80 °C.

Ten 2-fold serial dilutions were made from each lysate. The first dilution (four-fold dilution from the original lysate) was made with buffer containing 5 M urea, 2% Pharmalyte, pH 8–10.5, and 65 mM DTT. The remaining dilutions were then made with buffer containing 6 M urea, 1% CHAPS, 2% Pharmalyte, pH 8–10.5, and 65 mM DTT. Hence, only the lysate concentration changed along each dilution series. The urea concentration was thus kept at 6 M, and the CHAPS concentration at 2%, to keep proteins in their denatured forms. The lowest concentration dilution has a dilution factor of 2^{-11}.

2.2. Design and production of protein lysate array

Protein lysates were spotted onto nitrocellulose-coated glass slides (Nitrocellulose Film-Slides, Grace Bio-Labs,

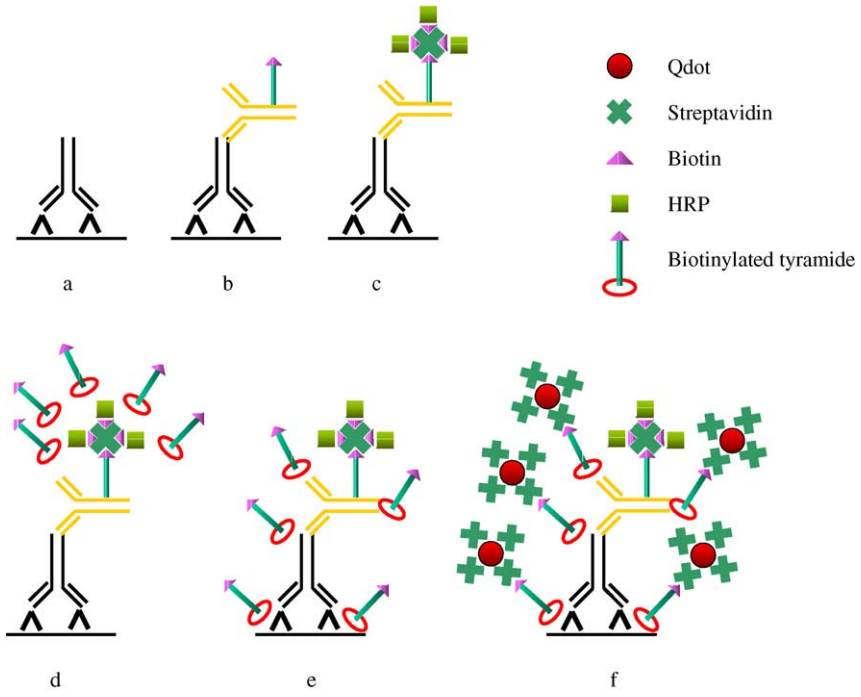

Fig. 1. Schematic overview of detection system using TSA and Qdots–streptavidin. (a) Primary antibody binds antigen. (b) Biotinylated secondary antibody binds primary antigen. (c) Streptavidin-biotin-HRP complex binds the biotin labeled on the secondary antibody. (d) Biotinylated tyramide is converted by HRP into a highly reactive oxidized intermediate. (e) Converted tyramide binds rapidly and covalently to cell-associated proteins at or near the HRP-linked antibody. (f) Qdots–streptavidin binds to the biotin on the tyramide.

Inc., Bend, OR, USA). Spotting was performed on an OmniGrid II high-speed microarray spotter (GeneMachines, San Carlos, CA, USA, now Genomic Solutions, Ann Arbor, MI, USA) with four 335 μm-diameter Stealth pins (TeleChem International, Inc., Sunnyvale, CA, USA). Spot-to-spot pitch distance is 500 μm. Extensive sonication washing and rinsing was carried out between spotting of different samples, to avoid carry-over cross-contamination. Fig. 3 shows the spot image of one of the arrays. Six repeats were printed for each dilution.

2.3. Qdot probe synthesis

The synthesis of CdSe/ZnS Qdots follows the procedures described in the literature [20]. We use CdSe cores of ∼2.5 nm with emission at 556 nm. In order to make them water-soluble, the Qdots are embedded into a cross-linked silica shell [32,33] and subsequently suspended in 10 mM PBS buffer, pH ∼7. The silica shell does provide the functional groups to perform bioconjugation. In particular, it contains over 100 thiol groups. We covalently link streptavidin-maleimide (Sigma-Aldrich) to the Qdots by incubating them together at the molar ratio 2:1, in 10 mM phosphate buffer, 50 mM NaCl for ∼1 to 2 h (Fig. 2A). The samples are cleaned from excess of STV by four rounds of centrifugation through Centricon 100 devices. The incorporation of streptavidin to the Qdots is probed by 1% agarose gel, where STV-Qdots display a lower mobility than bare Qdots due to their larger size (Fig. 2B). The final absorption and emission spectra of STV-Qdots is shown in Fig. 2C.

2.4. Detection of specific protein on microarrays

Each slide was washed manually with deionized water for 10 min to remove urea, then blocked with 1% I-block (Tropix, Bedford, MA, USA) in TBS buffer with Tween 20 (300 mM NaCl, 0.1% Tween 20, 50 mM Tris, pH 7.6) for 16 h overnight. Then, in an Autostainer universal staining system (DakoCytomation, Carpinteria, CA, USA), it was blocked for endogenous peroxidase, avidin, biotin and protein activity and incubated with primary and biotinylated secondary antibodies, following the vendor's instructions for immunohistochemistry staining. Also in the Autostainer, it was then incubated with the streptavidin–biotin complex and biotinylated tyramide (for amplification), each for 15 min, and by Qdot–streptavidin conjugates for 30 min. Between the steps, the slide was washed with TBS buffer with Tween 20 (300 mM NaCl, 0.1% Tween 20, 50 mM Tris, pH 7.6). Qdot–streptavidin conjugates were used at a 6.7 nM concentration diluted in 50 mM Borate, 2% BSA, pH 8.3, in a volume of 300 μL. To compare with the established method of reverse phase protein array lysate microarray with DAB, incubation with streptavidin-HRP for 15 min and with DAB for 5 min were performed after biotinylated tyramide was added. Monoclonal antibody against DNA-PKcs was used at a 1:10 dilution, the anti-

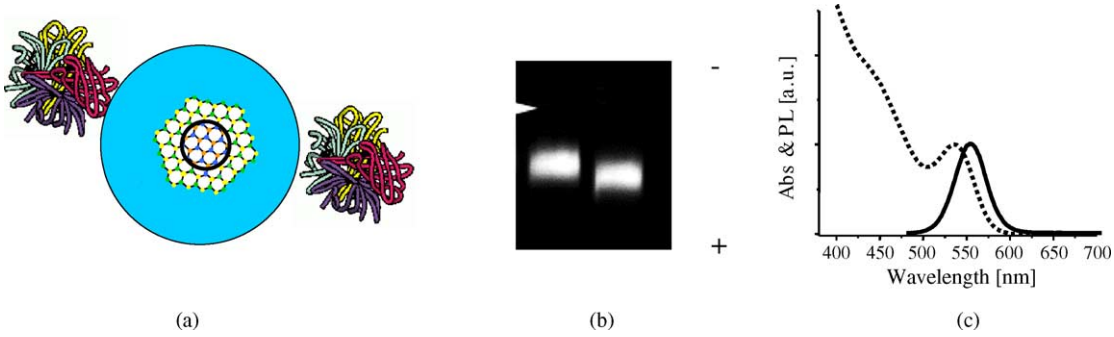

Fig. 2. (a) Schematics of the STV-Qdots, with two STV per Qdot. CdSe/ZnS Qdots are embedded in a functionalized silica shell terminating with thiols groups. Streptavidin-maleimide is covalently linked to the silica shell using the maleimide-thiol chemistry. Silica-coated Qdots are about 8 nm in size and STV is about 5–6 nm, so the schematics represent the relative size of the complex. (b) The coupling of the STV to the Qdots is confirmed by a 1% agarose gel (0.5× TBE, 16 V/cm for 30 min). Because of their emission, Qdots are easily seen in a transilluminator. STV-Qdots migrate less than silanized Qdots because of their greater size. The anode is at the bottom of the gel and the loading well is indicated by the white mark. If the maleimide of the STV is first hydrolyzed, the STV does not modify the Qdot mobility (not shown) indicating that there is no non-specific binding between the Qdot and streptavidin. (c) Absorption (dot line) and emission line (solid line, 556 nm, fwhm ∼32 nm) of the STV-Qdot conjugates. Note the continuous absorption from the band-edge down, which allows the excitation of the Qdot at every wavelength below ∼540 nm.

body being produced by hybridoma cell line 18-2 [27,28] and the dilution equivalent to a 1 mg/L final concentration.

2.5. Image analysis

In order to detect Qdot signals, a slide stained with Qdot–streptavidin has been scanned with a GenePix 4000A scanner (Axon Instruments, Union City, CA, USA) and saved as a TIFF file. Saturated signal intensity was 65535. GenePix has dual laser excitation, and collects emission at 532 nm (green) and 635 nm (red). Scanned images were analyzed and the relative fluorescence unit (RFU) was calculated with ImageQuant (Molecular Dynamics, CA) (Amersham Pharmacia Biotech, NJ) by using histogram peak background correction.

3. Results and discussion

Cell lysate from human glioma cell line M059J was used for the study, a cell line which is deficient in DNA-PKcs protein [27]. The cell lysate from M059J provides an appropriate proteome background that is representative of the general human cellular protein background, except that it lacks the target protein of this study, DNA-PKcs [29]. We spiked the lysate with DNA-PKcs protein purified from HeLa cells [30]. The DNA-PKcs was spiked into the undiluted M059J cell lysate at a concentration of 200 ng/ml, after a 1:4 initial dilution, the concentration of DNA-PKcs protein is 50 ng/ml, or ∼100 pM, which is the concentration reflected in the top rows of arrayed spots in Fig. 3a and b. The DNA-PKcs detection sensitivity limit achieved with the standard HRP–DAB assay is about 1 pM. The lysate has been further diluted in two-fold

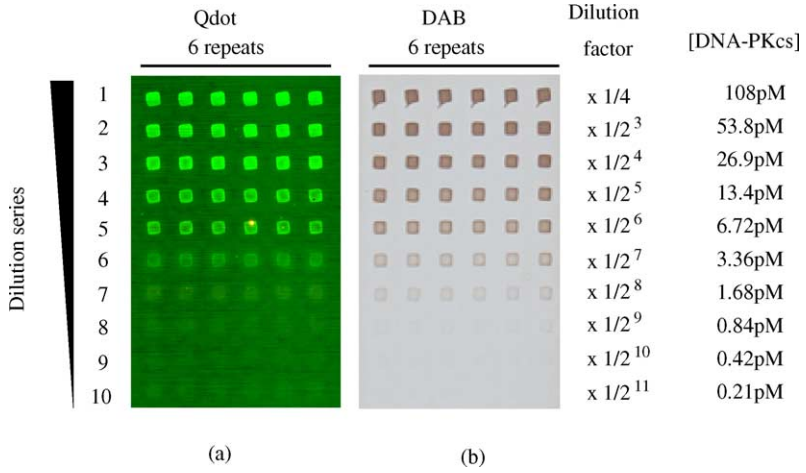

Fig. 3. Spot image of reverse phase protein microarray. Each column consists of 10 two-fold dilutions of protein DNA-PK-spiked lysate of M059J cells. There are six repeats at each dilution point. (a) Qdot staining. (b) DAB staining.

series down to 2^{-11} dilution factor, effectively extending the dynamic range to be ~1000 (=2^{10}). The Qdot signals on the protein array have been detected as shown in Fig. 3a. The Qdot method (Fig. 3a) shows a comparable sensitivity range as the HRP–DAB data (Fig. 3b). Spots from the first to the fifth dilutions can be comfortably detected with both Qdot and DAB methods. Both Qdot and HRP–DAB chemistry have been able to show detectable signals for the sixth and the seventh dilutions. Therefore, the Qdot-based assay is comparable in sensitivity to the standard commercial method based on HRP–DAB chemistry (Fig. 3). Indeed, after quantification of the fluorescent signal from Qdot and the colorimetric deposition of oxidized DAB, both the dynamic range and absolute sensitivity of the Qdot method and DAB method are within the same order of magnitude (Figs. 4 and 5).

Image analysis (Fig. 4) shows a good linearity between relative fluorescence unit and relative dilution in log-scale with a correlation coefficient of R^2 of 0.988. This result indicates that the combination of TSA and Qdots–streptavidin is suitable for protein quantification. Likewise, the DAB method also shows a good linear relationship between relative color unit (RCU) and relative dilution in log-scale, with a correlation coefficient of R^2 of 0.985 (Fig. 4b). In the detection procedure after biotin tyramide was added, different staining protocols have been used for the Qdot and the HRP–DAB method. To be more precise, in the Qdot method, only Qdot–streptavidin has been added. By contrast, in the HRP–DAB method, both streptavidin-HRP and DAB have been added. But when we compare directly the results of the Qdot method with that of the DAB method at each dilution point, the Qdot results show a good linearity with a correlation coefficient of R^2 of 0.986. From the viewpoint of protein quantification, these results provide evidence that, when combined with TSA, the use of Qdots is applicable to reverse phase protein microarray as effectively as is the standard HRP–DAB approach.

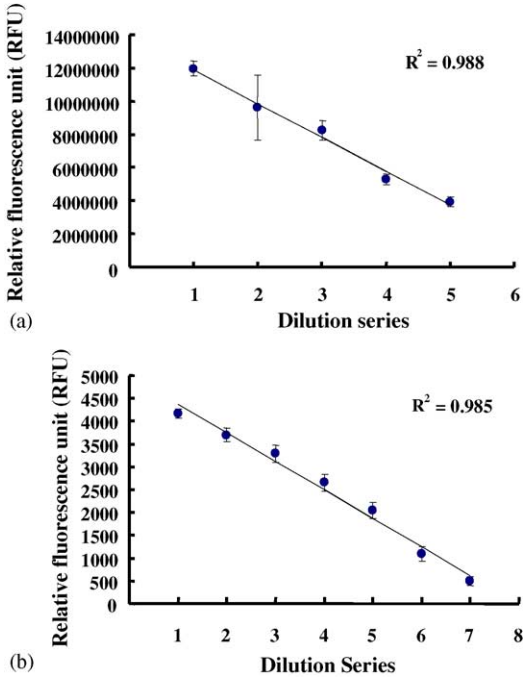

Fig. 4. Linear correlation with signal intensity and relative concentration in log-scale. Each spot at each dilution point shows average of RFU from six repeats and standard deviation as error bars. (a) A good linear correlation is shown in Qdots experiment (R^2 = 0.988). (b) A good linear correlation is shown in DAB experiment (R^2 = 0.985). Even though we can detect visually the spots up to the 8–10th dilution in Qdot-based assay in Fig. 3 with naked eye, the analysis software cannot translate the visual differences into accurate, quantitative numbers with good R values, due to the background fluorescent noise (see text).

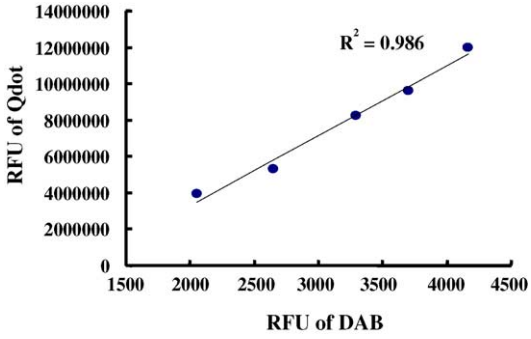

Fig. 5. Correlation of signal intensity between Qdots and DAB method. At five dilution points, both signal intensities were compared. A good linear correlation is shown between them (R^2 = 0.986).

Although the DAB method can detect spots up to the seventh and even the eighth dilution points, Qdot method has visualization of spots above the background signal up to the 10th dilution (Fig. 4a and b). However, we have only been able to extract data from the fifth dilution for the Qdot, due mainly to the algorithmic limitation of the ImageQuant software, which is more suitable for grayscale image (HRP–DAB) processing than for the RGB images (streptavidin–Qdot). This does not by any means indicate that the DAB method is two to four times as sensitive as Qdot. The discrepancy could also be partly due to the difference in signal-to-noise ratio between the Qdot and DAB methods. The intensity of the background in the Qdot method is much higher, which might be caused by non-specific binding of the streptavidin-coated Qdot. The colloidal nature of the Qdot makes it more vulnerable to precipitation and aggregation, which we have observed previously with our DNA microarray report [8]. Several possible solutions could improve the signal-to-noise ratio in the Qdot method. For example, to reduce the background, we can change the type of surface coating, for example, to a PEG-derived coating [34], in substitution of the nitrocellulose-coated glass slides, although we would then be trading protein-binding capacity for lower background. Further modifications in the surface coating of the Qdots, for the purpose of increasing solubility of the Qdots, may also help to prevent aggregation of the Qdots on the microarray substrate surface. We could also use near infrared wavelengths for Qdot excitation and emission. Calvert et al. reported

that in their multiple dye experiment, background autofluorescence from the nitrocellulose and cellular material was dramatically lower at infrared wavelengths than at visible wavelengths. They reported that they could reduce background fluorescence of nitrocellulose at both 700 nm and 800 nm emission wavelengths in the near infrared spectra, when compared to visible wavelengths [35]. This suggests that, instead of the wavelength of 532 nm for Qdot detection, we could use Qdots that emit at infrared wavelengths. Looked at in another way, optimizing Qdot concentration for hybridization may give us a stronger signal as described in the literature, where it has been reported that increasing the concentration of Qdot nanoconjugates up to 20 nM could result in signal enhancement [36]. Thus, there still remains the potential for improving sensitivity in the Qdots method.

In addition to its capability in quantifying protein, Qdots have good photostability (Fig. 6) [32], and narrow emission patterns, which will be an advantage for multiplex detection of proteins and the ability to conjugate with a wide variety of biomolecules such as antibody [32]. The photostability is useful in maintaining a constant fluorescent signal during multiple scans, making the quantification more accurate. In addition, the photostability makes short-term archiving of the protein microarray possible. In the case of the colorimetric assay, the chromogenic compound will have darkened color only after a few hours, because DAB is sensitive to environmental oxidative stresses. Additionally, environmental variations such as temperature and humidity will affect the color development speed and the signal strength of DAB, introducing variations in assay readout.

Another factor affecting data reproducibility is the quality of the protein array printing. Unlike DNA microarrays, in which dual-color labeling can be used to correct variations between arrays, the reverse phase protein array can only provide relative expression levels for the protein on one array at a time. We discovered that the best printing mechanism would be using non-contact printing for protein array, because the deposited volume of protein lysate can be well controlled using a system such as piezo-electric delivery. Our data has shown good reproducibility between the repeat spots of the same sample, all achieved at a high density of at least 400 spotted features/cm^2 of protein lysate array.

In conclusion, to quantify protein lysate, we have developed a procedure using TSA and Qdot–streptavidin on protein microarrays. Our results indicate that we can use combination of TSA and Qdots–streptavidin to quantify protein, and the data agree very closely with standard HRP–DAB colorimetric data. We believe that we can extend our results to the quantification of protein in many areas, such as cell imaging, protein interaction assays, and pathogen detection.

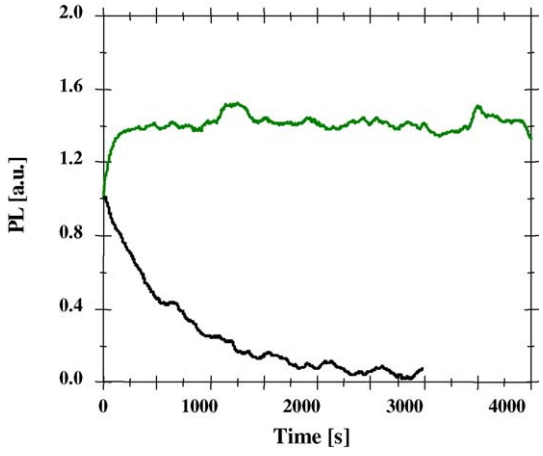

Fig. 6. Stability of Qdots vs. organic dyes under continuous laser radiation (3 mW/cm^2) in a 1 mm^3 cuvette. Qdots show stable emission over hours, while rhodamine 6G bleaches after less than 10 min. Similar behaviors are observed for Qdots and dyes dried on surfaces. Over repeated scans, the dyes bleach but the Qdots maintain their emission level. Adapted from authors' other work [32].

Acknowledgements

We thank Mr. Kevin Peet for excellent administrative support, we also thank Johnathan Zhang, Shota Yamamoto, and Dustin Dean for excellent technical support. We thank Drs. Steve Yannone and Benjamin P. Chen for providing antibody to target proteins, Drs. N. Zaitseva and G. Galli for their support, and Prof. A.P. Alivisatos for access to his laboratory. This work was supported by NIH Grant R21CA95393-01, by NASA grant NNA04CA75I, by Department of Energy grant to F. Chen and by NIH P50 grant CA112970 to J.W. Gray. This work was performed under the auspices of the U.S. Department of Energy, at the University of California/Lawrence Livermore National Laboratory under contract no. W-7405-Eng-48, and at the University of California/Lawrence Berkeley National Laboratory under contract no. DE-AC03-76SF00098.

References

[1] M.F. Templin, D. Stoll, M. Schrenk, P.C. Traub, C.F. Vohringer, T.O. Joos, Trends Biotechnol. 20 (2002) 160.
[2] H. Zhu, M. Bilgin, R. Bangham, D. Hall, A. Casamayor, P. Bertone, N. Lan, R. Jansen, S. Bidlingmaier, T. Houfek, T. Mitchell, P. Miller, R.A. Dean, M. Gerstein, M. Snyder, Science 293 (2001) 2101.
[3] G. MacBeath, S.L. Schreiber, Science 289 (2000) 1760.
[4] G. MacBeath, Nat. Genet. 32 (Suppl.) (2002) 526.
[5] E. Phizicky, P.I. Bastiaens, H. Zhu, M. Snyder, S. Fields, Nature 422 (2003) 208.
[6] D.J. Cutler, M.E. Zwick, M.M. Carrasquillo, C.T. Yohn, K.P. Tobin, C. Kashuk, D.J. Mathews, N.A. Shah, E.E. Eichler, J.A. Warrington, A. Chakravarti, Genome Res. 11 (2001) 1913.
[7] D. Altshuler, L. Kruglyak, E. Lander, N. Engl. J. Med. 338 (1998) 1626.
[8] D. Gerion, F. Chen, B. Kannan, A. Fu, W.J. Parak, D.J. Chen, A. Majumdar, A.P. Alivisatos, Anal. Chem. 75 (2003) 4766.
[9] P.Y. Kwok, Pharmacogenomics 1 (2000) 95.
[10] T.D. Lacoste, X. Michalet, F. Pinaud, D.S. Chemla, A.P. Alivisatos, S. Weiss, Proc. Natl. Acad. Sci. U.S.A. 97 (2000) 9461.

[11] S. Raychaudhuri, P.D. Sutphin, J.T. Chang, R.B. Altman, Trends Biotechnol. 19 (2001) 189.
[12] C.P. Paweletz, L. Charboneau, V.E. Bichsel, N.L. Simone, T. Chen, J.W. Gillespie, M.R. Emmert-Buck, M.J. Roth, I.E. Petricoin, L.A. Liotta, Oncogene 20 (2001) 1981.
[13] L.A. Liotta, V. Espina, A.I. Mehta, V. Calvert, K. Rosenblatt, D. Geho, P.J. Munson, L. Young, J. Wulfkuhle, E.F. Petricoin III, Cancer Cell 3 (2003) 317.
[14] V. Espina, E.C. Woodhouse, J. Wulfkuhle, H.D. Asmussen, E.F. Petricoin III, L.A. Liotta, J. Immunol. Methods 290 (2004) 121.
[15] M.N. Bobrow, T.D. Harris, K.J. Shaughnessy, G.J. Litt, J. Immunol. Methods 125 (1989) 279.
[16] M.N. Bobrow, K.J. Shaughnessy, G.J. Litt, J. Immunol. Methods 137 (1991) 103.
[17] B. Hunyady, K. Krempels, G. Harta, E. Mezey, J. Histochem. Cytochem. 44 (1996) 1353.
[18] G. King, S. Payne, F. Walker, G.I. Murray, J. Pathol. 183 (1997) 237.
[19] P. Alivisatos, Nat. Biotechnol. 22 (2004) 47.
[20] B.O. Dabbousi, J. RodriguezViejo, F.V. Mikulec, J.R. Heine, H. Mattoussi, R. Ober, K.F. Jensen, M.G. Bawendi, J. Physical Chem. B 101 (1997) 9463.
[21] S. Pathak, S.K. Choi, N. Arnheim, M.E. Thompson, J. Am. Chem. Soc. 123 (2001) 4103.
[22] B. Dubertret, P. Skourides, D.J. Norris, V. Noireaux, A.H. Brivanlou, A. Libchaber, Science 298 (2002) 1759.
[23] W.C. Chan, S. Nie, Science 281 (1998) 2016.
[24] X. Wu, H. Liu, J. Liu, K.N. Haley, J.A. Treadway, J.P. Larson, N. Ge, F. Peale, M.P. Bruchez, Nat. Biotechnol. 21 (2003) 41.
[25] J.K. Jaiswal, H. Mattoussi, J.M. Mauro, S.M. Simon, Nat. Biotechnol. 21 (2003) 47.
[26] M.E. Akerman, W.C. Chan, P. Laakkonen, S.N. Bhatia, E. Ruoslahti, Proc. Natl. Acad. Sci. U.S.A. 99 (2002) 12617.
[27] S.R. Peterson, M. Stackhouse, M.J. Waltman, F. Chen, K. Sato, D.J. Chen, J. Biol. Chem. 272 (1997) 10227.
[28] F. Chen, S.R. Peterson, M.D. Story, D.J. Chen, Mutat. Res. 362 (1996) 9.
[29] S.P. Lees-Miller, R. Godbout, D.W. Chan, M. Weinfeld, R.S. Day III, G.M. Barron, J. Allalunis-Turner, Science 267 (1995) 1183.
[30] S.R. Peterson, S.A. Jesch, T.N. Chamberlin, A. Dvir, S.K. Rabindran, C. Wu, W.S. Dynan, J. Biol. Chem. 270 (1995) 1449.
[31] S. Nishizuka, L. Charboneau, L. Young, S. Major, W.C. Reinhold, M. Waltham, H. Kouros-Mehr, K.J. Bussey, J.K. Lee, V. Espina, P.J. Munson, E. Petricoin III, L.A. Liotta, J.N. Weinstein, Proc. Natl. Acad. Sci. U.S.A. 100 (2003) 14229.
[32] D. Gerion, F. Pinaud, S.C. Williams, W.J. Parak, D. Zanchet, S. Weiss, A.P. Alivisatos, J. Physical Chem. B 105 (2001) 8861.
[33] W.J. Parak, D. Gerion, D. Zanchet, A.S. Woerz, T. Pellegrino, C. Micheel, S.C. Williams, M. Seitz, R.E. Bruehl, Z. Bryant, C. Bustamante, C.R. Bertozzi, A.P. Alivisatos, Chem. Mater. 14 (2002) 2113.
[34] T. Cha, A. Guo, Y. Jun, D. Pei, X.Y. Zhu, Proteomics 4 (2004) 2823.
[35] V.S. Calvert, Y. Tang, V. Boveia, J. Wulfkuhle, A. Schutz-Geschwender, D.M. Olive, L.A. Liotta, E. Petricoin III, Clin. Proteomics J. 1 (2004) 81.
[36] J.M. Ness, R.S. Akhtar, C.B. Latham, K.A. Roth, J. Histochem. Cytochem. 51 (2003) 981.